J Fluoresc (2009) 19:21–31
DOI 10.1007/s10895-008-0375-5

ORIGINAL PAPER

Phosphate Assisted Proton Transfer in Water and Sugar Glasses: A Study Using Fluorescence of Pyrene-1-carboxylate and IR Spectroscopy

Bogumil Zelent · Jane M. Vanderkooi · Nathaniel V. Nucci · Ignacy Gryczynski · Zygmunt Gryczynski

Received: 12 March 2008 / Accepted: 10 April 2008 / Published online: 22 May 2008

Abstract The role of water's H-bond percolation network in acid-assisted proton transfer was studied in water and glycerol solutions and in sugar glasses. Proton transfer rates were determined by the fluorescence of pyrene-1-carboxylate, a compound with a higher pK in its excited state relative to the ground state. Excitation of pyrene-1-COO^- produces fluorescence from pyrene-1-COOH when a proton is accepted during the excited singlet state lifetime of pyrene-1-COO^-. The presence of glycerol as an aqueous cosolvent decreases proton transfer rates from phosphoric and acetic acid in a manner that does not follow the Stokes relationship on viscosity. In sugar glass composed of trehalose and sucrose, proton transfer occurs when phosphate is incorporated in the glass. Sugar glass containing phosphate retains water and it is suggested that proton transfer requires this water. The infrared (IR) frequency of water bending mode in sugar glass and in aqueous solution is affected by the presence of phosphate and the IR spectral bands of all phosphate species in water are temperature dependent; both results are consistent with H-bonding between water and phosphate. The fluorescence results, which studied the effect of cosolvent, highlight the role of water in assisting proton transfer in reactions involving biological acids, and the IR results, which give spectroscopic evidence for H-bonding between water and phosphate, are consistent with a mechanism of proton transfer involving H-bonding. The possibility that the phosphate-rich surface of membranes assists in proton equilibration in cells is discussed.

Keywords Proton transfer · Phospholipids · Membranes · Water · Percolation · Glycerol

B. Zelent · J. M. Vanderkooi (✉) · N. V. Nucci
Department of Biochemistry and Biophysics, School of Medicine, University of Pennsylvania,
Philadelphia, PA 19104, USA
e-mail: vanderko@mail.med.upenn.edu

I. Gryczynski · Z. Gryczynski
Center for Commercialization of Fluorescence Technologies, Health Science Center, University of North Texas,
3500 Camp Bowie Blvd.,
Fort Worth, TX 76107, USA

Introduction

Proton transfer rates in living cells are highly regulated. Trans-membrane proton transfer is coupled with energy production, whereas proton transfer in the aqueous cellular solutions must be fast. Proton transfer rates in water are enhanced by water's ability to be both an H-bond donor and acceptor, with the result that hydronium ions diffuse faster than the diffusion of water molecules [1]. This well-accepted process is called the Grotthuss mechanism, named for the researcher who reported early proton diffusivity measurements [2].

In this paper we are examining the role of water's H-bonding network in influencing proton transfer rates under conditions where the water network is disrupted. Proton transfer rates are monitored using the fluorescence of pyrene-1-COO^-, a compound that is more basic in its singlet-excited state relative to ground state. The difference in pK between ground and excited state molecules is rationalized by quantum calculations demonstrating that the aromatic character of the bond between the ring system and carboxyl group becomes stronger in the excited state [3]. From fluorescence spectra and lifetimes, proton transfer rates can be determined. Previously, we showed that water

at neutral pHs does not provide a proton to pyrene-1-COO^{-}* but a proton could be transferred from acetic and phosphoric acids in the aqueous solution [4]. Phosphate is the physiological buffer of living systems; acetate contains a carboxyl group; this functional group also serves as a biological buffer and carboxy-groups are found on surfaces of proteins and in intermediary metabolites. We gave evidence that phosphate, like water, accelerates rates of proton transfer by virtue of its ability to be both a proton donor and acceptor [4].

The experiments are divided into four aspects. First, to investigate the role of the water network we determine rates of proton transfer from phosphoric and acetic acids where water's H-bond network is disrupted by the addition of glycerol. Our laboratory group previously examined water/glycerol solutions by infrared (IR) and computation [5, 6]; the computations showed that glycerol affects the H-bonding pattern of water at low concentrations, and that the H-bond percolation network of water is disrupted at high concentrations. Second, the temperature dependence of the reaction is studied in order to separate proton transfer via diffusion of proton donors or from transfer via the H-bond network. Third, to demonstrate the role of the water–phosphate complex in proton transfer reactions we use sugar glasses that have varying amounts of water and are doped with proton donors. Water content of sugar glasses can be determined by IR spectroscopy [7] and proteins have been incorporated in sugar glasses with retention of conformation [7, 8]. Because of these reasons, sugar glasses are a good model to study the role of water in proton transfer. It is shown that the OH stretching frequency of water is affected by the presence of phosphate both in sugar glass and in aqueous solution, supporting the idea that phosphate participates in the H-bond network. Finally, IR spectroscopy was used to examine the effect of water on phosphate. We present the IR spectra of all phosphate forms as a function of temperature. As temperature decreases H-bonding strength increases [9]; the changes in the bending and stretching frequencies of phosphate are strong evidence of H-bonding interactions between phosphate and water.

Materials and methods

Materials

Water was deionized and then glass distilled. Pyrene-1-carboxylic acid was obtained from Fluka Chemie GmbH (Deisenhofen, Germany). Na_2HPO_4-$7H_2O$, NaH_2PO_4 and Na-acetate were Baker analyzed reagent grade. Spectral grade glycerol was obtained from Sigma Company. The pHs of solutions were measured using a glass electrode that was calibrated with standard buffers. All samples were equilibrated with atmosphere.

Preparation of sugar glasses

Sugar film was prepared as previously described [8]. Stock sugar solution or sugar solution containing Na-acetate or Na-phosphate at pH 5.0 was plated on a CaF_2 plate (Janos Technology). The samples were allowed to dry for >3 h at 65 °C for "dehydrated" samples. During drying, the sample temperature was maintained using a VWR Scientific Products Heat Block. For "hydrated" samples the samples were maintained at 65 °C for 30 min, and allowed to sit in the atmosphere. The resulting sugar films were ~6–20 μm in thickness. Infrared spectra were taken of samples; this allows evaluation of the ratio of water to sugar in the glass [7]. The "dehydrated" glasses made without phosphate or acetate and sugar glass containing acetate had no IR-detectible water remaining. Phosphate-containing sugar retained water even after "dehydration" conditions. The hydrated sugar samples contained about one water molecule/sugar molecule. The IR spectra of the sugar containing acetate showed the symmetric and anti-symmetric stretches of the carboxylate, showing that acetate retained the protonation state in the glass that it had in the starting solution

Absorption, fluorescence and IR spectroscopy

A Hitachi Perkin-Elmer U-3000 absorption instrument (Hitachi Instruments Inc., Danbury, CT, USA) was used to take ultraviolet-visible absorption spectra.

Fluorescence emission spectra were measured with a Fluorolog-3-21 Jobin-Yvon Spex Instrument SA (Edison, NJ, USA) equipped with a 450 W Xenon lamp for excitation and a cooled R2658P Hamamatsu photomultiplier tube for detection. Slit width was set to provide a band-pass of 2 nm for excitation and for emission. The concentration of pyrene-1-carboxylate was adjusted to give an absorbance of 0.05 at the excitation wavelength, 333 nm. Measurements used 90° geometry.

Infrared spectra were obtained with a Bruker IFS 66 Fourier transform IR spectrophotometer (Bruker, Brookline, MA, USA). The sample compartment and optical path were purged with nitrogen to reduce the contribution from atmospheric carbon dioxide and water vapor. The signal was monitored using an HgCdTe detector. The sample temperature was regulated using a Neslab RTE 740 water bath (Thermo Electron Corp., Waltham, MA, USA) and was monitored using a Fisherbrand Traceable Total-Range digital thermometer (Fisher Scientific International Inc., Hampton, NH, USA). All spectra were taken in transmission mode with an aperture of 2.0 mm and a spectral

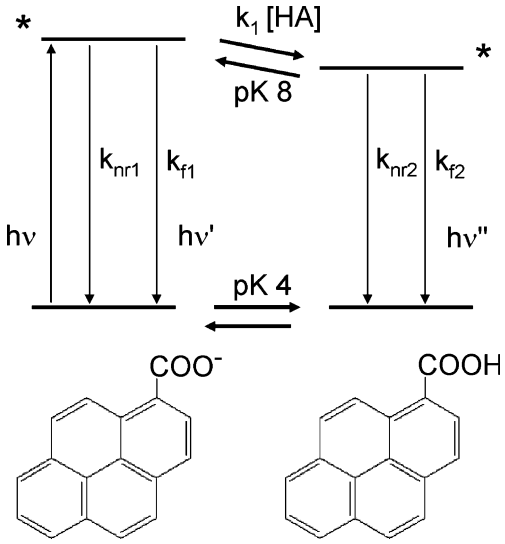

Fig. 1 Scheme for excited state protonation. Ground and excited state pKs of pyrene-1-COOH are indicated. Non-radiative decay rates are indicated by k_{nr} and fluorescence decay rates by k_f. The bimolecular rate of protonation is indicated by k_1

resolution of 2 cm^{-1}. CaF_2 windows were used for the measurement of sugars and ZnSe windows were used for the measurement of phosphate. Before measurement of the sample spectra, the transmission spectrum of atmosphere (i.e., water vapor and CO_2) and windows without the sample was taken for reference. Spectra were processed for water vapor and CO_2 compensation, for baseline correction, nine-point Savitsky–Golay smoothing, and conversion to absorbance using OPUS v. 5.0 software (Bruker).

Fluorescence lifetime measurements

Fluorescence intensity decays were measured using the time-correlated single-photon-counting FluoTime200 fluorimeter (PicoQuant, Inc., Berlin, Germany). This instrument has a pulsed 334 nm light-emitting diode for excitation and uses magic angle polarizer orientation to avoid effects of Brownian rotation. Emitted light was selected using a monochromator. A microchannel plate is the detector and the data were fitted with FluoFit software (PicoQuant, version 4). The lifetime is obtained from the time course of the intensity:

$$I(t) = Ae^{t/\tau} \quad (1)$$

where A is the initial amplitude of intensity and τ is the lifetime. The observed rate constant, $k_f = 1/\tau$.

Data analysis to obtain proton transfer rates

Figure 1 gives the reaction diagram. The experiments were usually carried out at pH 5.0. Therefore, most of the pyrene derivative is in the carboxylate form. As seen in the diagram, whether fluorescence originates from pyrene-1-COO^-* or pyrene-1-COOH* depends on the rate of protonation and the rate of fluorescence decay. Protonation of pyrene-1-COO* results in a quenching of its fluorescence. Data for fluorescence lifetimes are given in Table 1. The fluorescence decay can be described by a single exponential function, as indicated by reduced χ^2 values close to 1. The lifetime of pyrene-1-COO^- in glycerol solution was somewhat lower than for the water solution. In-as-much that O_2 quenches excited state pyrene [10], the lower lifetime in high glycerol may be due to higher concentration of O_2. Neither water nor glycerol provided a proton to pyrene-1-COO^-* as indicated by the fact that in either solvent excitation of the carboxylate did not produce emission of pyrene-1-COOH*. The fluorescence lifetime of pyrene-1-COOH is also given in Table 1. This lifetime is not involved in the calculation, except to note that it is much shorter than the lifetime of pyrene-1-COO^-. Its shorter lifetime, plus the lower energy of the emission of pyrene-1-COOH, relative to pyrene-1-COO^-, lessens the likelihood that the protonation reaction is reversible in the excited state.

The intensity, relative yields of acid and base forms and/or lifetimes were used to determine rate constants. Spectra were analyzed to give relative concentrations of acid and base forms based upon the emission spectra. The quantum efficiencies of pyrene-1-COO^- and pyrene-1-COOH were determined by taking the integrated intensity of samples adjusted to the same optical density at 333 nm. To obtain the integrated intensity, the fluorescence spectra were converted from wavelength to wave number, using literature accepted procedure and representation [11].

To calculate the unimolecular rate constants (i.e. rate at a given proton donor concentration), it was assumed that at a

Table 1 Fluorescence lifetimes of pyrene-1-COOH and pyrene-1-COO^- at 20 °C in water and glycerol

Compound	pH	Solvent	τ, ns	χ^2_R
pyrene-1-COOH	1.0	H_2O	4.9	0.95
pyrene-1-COO^-	10	H_2O	37	1.05
pyrene-1-COOH	1.0	50% glycerol	4.8	1.23
pyrene-1-COO^-	9.5	0% glycerol	37.1	1.04
		10% glycerol	35.3	1.01
		20% glycerol	34.3	1.01
		30% glycerol	33	1.01
		40% glycerol	31.7	1.01
		50% glycerol	30.5	0.98
		60% glycerol	29.3	0.99
		70% glycerol	28.4	1.00
		80% glycerol	27.7	1.01
		90% glycerol	27.2	1.28

given proton donor concentration the rate of decay of fluorescence, k_{obs} at a fixed [HA] concentration is:

$$k_{obs} = k_f + k_t \quad (2)$$

where k_f is the measured fluorescence decay rate in the absence of quencher. The rate of transfer, k_t is the simple difference between the two measured rates. This measurement is valid, since as noted above on Table 1, the decay function is single exponential. Equipment was not available to measure fluorescence lifetime at all temperatures, and so the observed rates k_{obs} were obtained from the temperature dependence of fluorescence intensity making the assumption that fluorescence intensity, F, is proportional to lifetime τ, i.e.:

$$F \alpha \tau$$

then

$$1/((F/F_o)*\tau_o) = 1/\tau_o + k_t \quad (3)$$

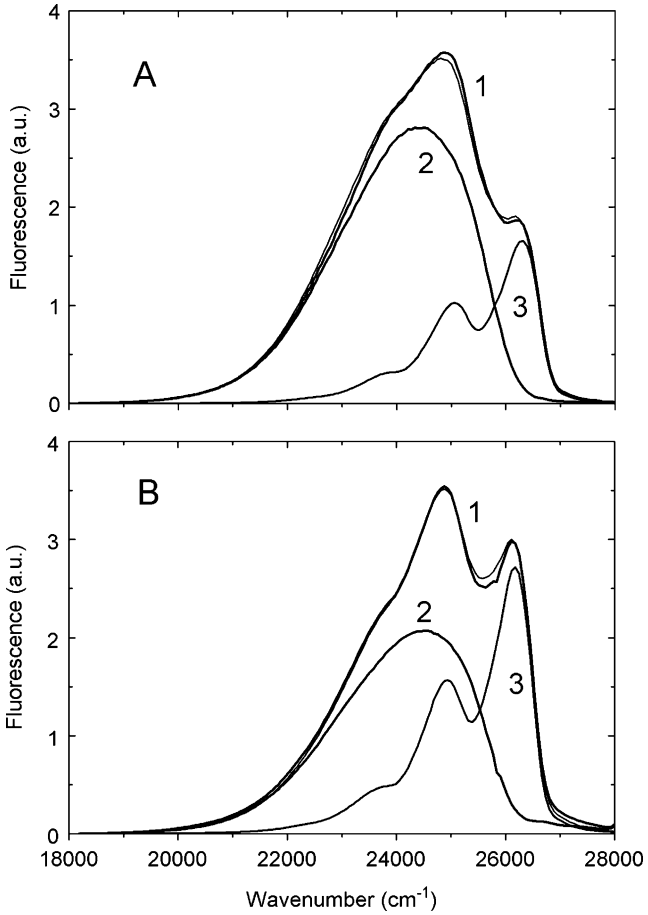

Fig. 2 Analysis of fluorescence emission spectra for contributions from pyrene-1-COO^- and pyrene-1-COOH. Dye concentration was 1 μM in: **a** water, **b** glycerol/water (1/1 *v/v*) at 20 °C. *Thin lines* are experimental spectra for: *1* pyrene–carboxylate in the presence of 1 M phosphate, sodium salt, pH 5; *2* pyrene-1-COOH at pH 1; *3* pyrene-1-COO^- at pH 9.0. *Thick lines* labeled *1* are the sum of the deconvolved spectra. The ratio of acid/base, based on integrated intensity, was 2.9 in water (**a**) and 1.4 in glycerol/water (**b**)

When bimolecular rate constants were determined, the Stern–Volmer relationship was used:

$$\tau_o/\tau = F_o/F = 1 + \tau_0 k_q[HA] \quad (4)$$

where k_q is the desired rate constant with units of per molar per second, [HA] is the concentration of the proton donor, and τ_o and F_o are the respective lifetimes and intensities (based upon integrated areas) for pyrene-1-COO^- fluorescence without added proton donors, i.e. without phosphate or acetate. In temperature dependence measurements it is difficult to obtain F_o and F fluorescence intensities relative to each other since a separate sample must be prepared for every temperature, and the sample cell cannot be positioned in the beam exactly the same from sample to sample. In these cases, the effective intensity for F_o was obtained as follows: the spectra were deconvolved for contributions of pyrene-1-COO^- and pyrene-1-COOH, and then the intensity of pyrene-1-COO^- was calculated to what it would be if no pyrene-1-COOH had been formed. For every temperature and glycerol concentration spectra of pyrene-1-COO^- and pyrene-1-COOH were determined as a basis for the deconvolution.

Estimation of pK change with addition of glycerol

In our previous work we established that the acid form of the buffer is the proton donor [4]. Since the fluorescence measurements were made at pH values near or above the pK of the acid, the concentration of acid is calculated based upon the experimentally known salt concentration and its pK. To determine the concentration of the acid forms in water the following pKs were used: 2.12 for phosphate and 4.76 for acetate. The presence of glycerol can change the pK. To determine the pK values of the acids in glycerol, glycerol was added to the buffer and the pH change measured. Using the Henderson–Hasselbalch equation, we obtained pK values of 2.42 for phosphate and 5.0 for acetate in 1/1 (*v/v*) glycerol/water. Concentrations of the acid forms of the proton donors were calculated at pH 5.0 as $[H_3PO_4]$= 0.0026×[total phosphate salt] and [acetic acid]=0.5×[total acetate salt].

Results

Effect of glycerol on protonation rates

Emission spectra of pyrene-1-carboxylate in the presence of phosphate at pH 5 are given in Fig. 2a for aqueous solution without glycerol and in Fig. 2b for solution with glycerol. The deconvolved components of the spectra are also shown, to illustrate the analysis procedure. It can be seen that the contribution of the acidic form (label 2) is reduced

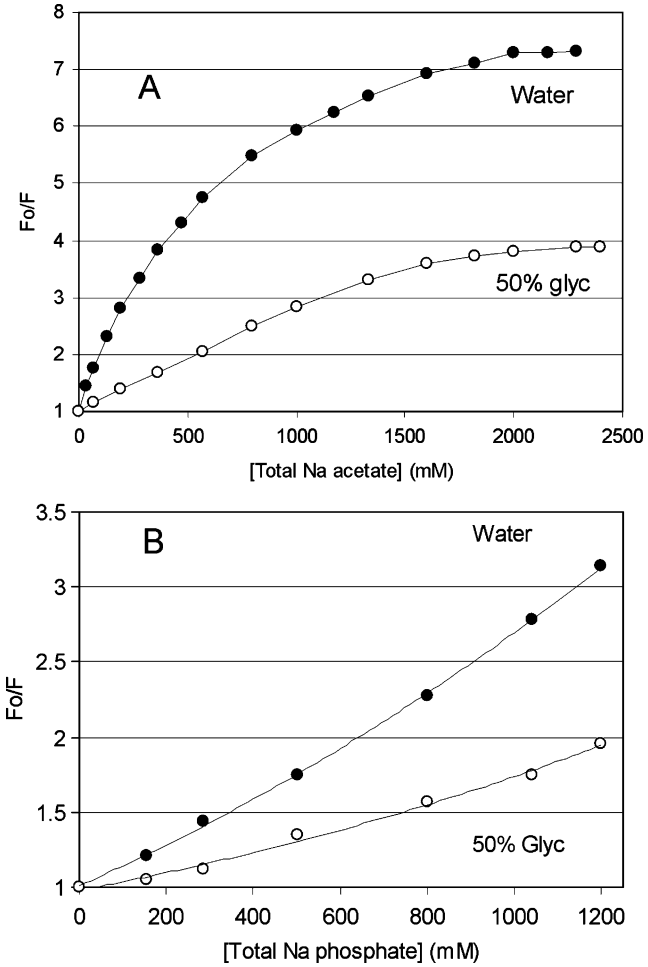

Fig. 3 Stern–Volmer plots of fluorescence yield of 1 μM pyrene-1-COO^- in the presence of acetate (**a**) and phosphate (**b**) at 20 °C at pH 5, in water (*closed circles*) and 1/1 *v*/*v* glycerol/water, i.e., 0.21 mol% (*open circles*). Fluorescence yield (F) relative to the yield in the absence of proton transfer (F_o) was calculated from deconvolved spectra as described in "Materials and methods" and Fig. 2

relative to the basic form (label 3) in the presence of glycerol. At the excitation wavelength used, the relative quantum yield of pyrene-1-COOH to pyrene-1-COO^- (based upon the integrated intensity of the acid and basic forms at extreme pHs) is 1.33. From the integrated intensities of the sample in Fig. 2a, F_o/F is 3.21 and in Fig. 1b F_o/F is 2.05. Not shown are the spectra of pyrene-1-COO^- at pH 5.0 in the respective solvents. The emission spectra showed no evidence of excited state proton transfer reaction, but a small component of pyrene-1-COOH* was seen, consistent with ground-state concentration of this species at this pH.

The fluorescence ratio F_o/F of the basic form is plotted following Eq. 4 for acetate and phosphate in Fig. 3a,b. The plot with acetate is linear at low concentrations but, at high concentration, it approaches a limiting rate. The rate over the entire concentration slows in the presence of glycerol. The titration with phosphate shows cooperative behavior, as previously noted [4]. Glycerol reduces the yield of protonation, but features of the titrations (i.e. limiting rate for acetate and cooperativity for phosphate) are maintained.

The unimolecular rates of reaction as a function of mole fraction of glycerol/ water are shown in Fig. 4. The unimolecular rate constants, based on Eq. 2 and the lifetimes presented in Table 1, are for 0.3 M Na acetate and 1 M Na phosphate, pH 5. The reaction rates of proton transfer from phosphoric and acetic acids decrease in glycerol cosolvent.

As glycerol concentration increases, there are more glycerol–glycerol interactions. The changes in molecular interactions are manifested as a change in viscosity. In the ideal case, the diffusion-controlled rate for large spherical molecules depends upon temperature and viscosity of the solvent by:

$$k = 8RT/3000\eta \qquad (5)$$

where η is the viscosity in Poise. Figure 5a presents the data shown in Fig. 4 but instead the transfer rate is plotted as a function of inverse viscosity. Although the absolute values for proton transfer differ for acetate and phosphate, the effect of glycerol is nearly the same. Both show non-ideal behavior; at high glycerol concentrations: the rate decreases more than predicted from viscosity-dependent diffusion alone. Experimental literature data showing the regimes of three dimensional and two dimensional networks based on physical measurements [12, 13] are also indicated in the figure. In Fig. 5b, computed H-bonding neighbors for water, based on the work of Dashnau et al. [5] are shown. The open squares represent water in the three-dimensional network, and it can be seen that at high

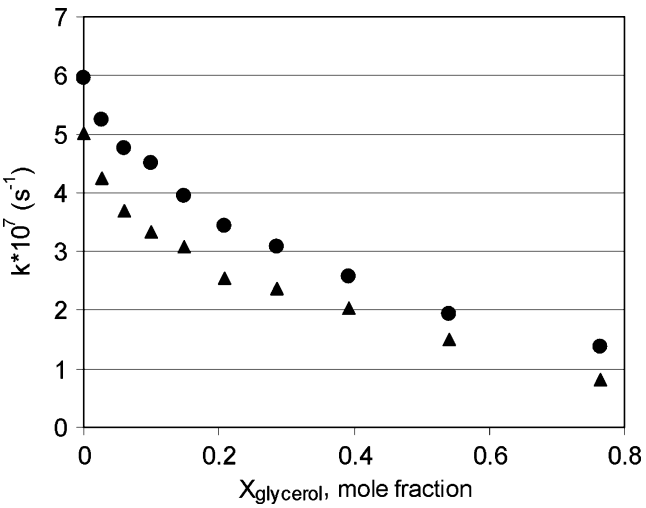

Fig. 4 Unimolecular rate of protonation of excited state pyrene-1-COO^- or fluorescence quenching as a function of mole fraction glycerol at 20 °C. Solution was at pH 5.0 and 1 M phosphate (*circles*), 0.25 M acetate (*triangles*) as sodium salts. The rate constant was calculated using deconvoluted spectra, measured fluorescence lifetimes (Table 1) and Eq. 2

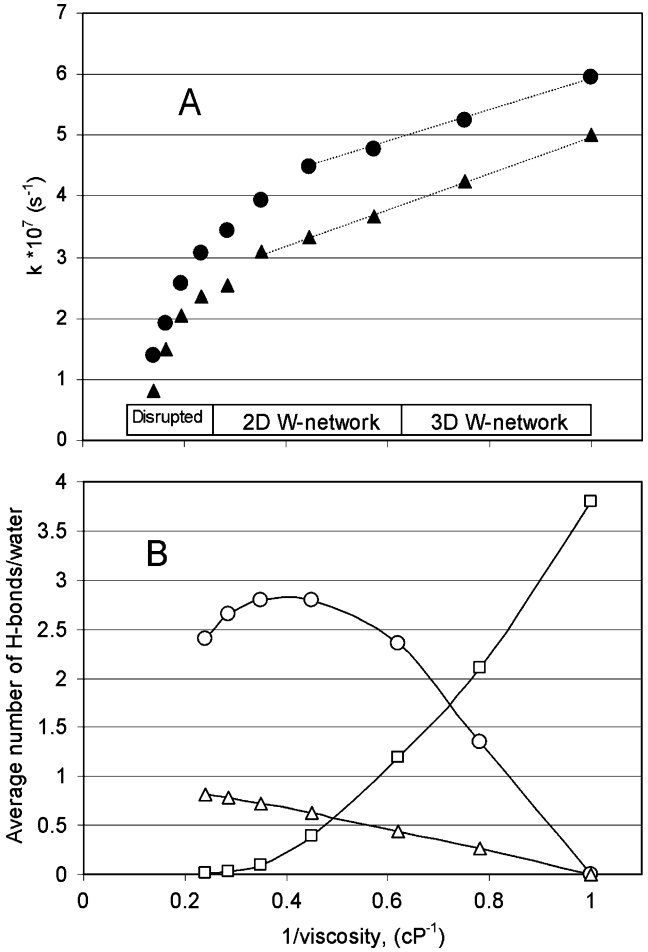

Fig. 5 **a** Unimolecular rate constant of pyrene-1-COO^- quenching by 1 M phosphate (*circles*) and 0.3 M acetate (*triangles*) at 20 °C as a function of reciprocal of viscosity (*cP*) of the glycerol–water system described in Fig. 4. *Bottom*: H-bonding network based on thermodynamic parameters [12, 13]. **b** Water H-bonding calculated based on glycerol concentration. *Squares* refer to water–water interactions and refers to bulk water; *circles* are waters involved in the solvation shell around glycerol and *triangles* are waters that are solely H-bonded to glycerol hydroxyl. Details are found in Dashnau et al. [5]

viscosity the network is decreased. One can see that the interruption of the three-dimensional water network coincides with decreased rate of proton transfer.

Effect of temperature

Reducing temperature decreases the proton transfer rate for reactions of acetic and phosphoric acids with pyrene-1-COO^-*. Spectra in Fig. 6a,b document changes in fluorescence as a function of temperature for the base and acid forms in the absence of excited-state proton transfer and provide spectra required for deconvolution of the spectra in the presence of proton transfer. The spectra of Fig. 6c show that in the presence of phosphate the yield of the protonated form decreases as temperature decreases.

If the reaction of excited state involves rearrangement of atoms, then the reaction can be described as a product of an efficiency factor, A, and the Boltzmann factor $-\Delta E/RT$, as expressed by the Arrhenius equation:

$$k = Ae^{-\Delta E/RT} \tag{6}$$

where R is the universal gas constant (R=8.314 JK^{-1} mol^{-1}), ΔE is the energy of activation and T is the Kelvin temperature.

Experimentally determined bimolecular rate constants for proton transfer are plotted in Fig. 7 as a function of reciprocal temperature according to Eq. 6. Equation 5 was

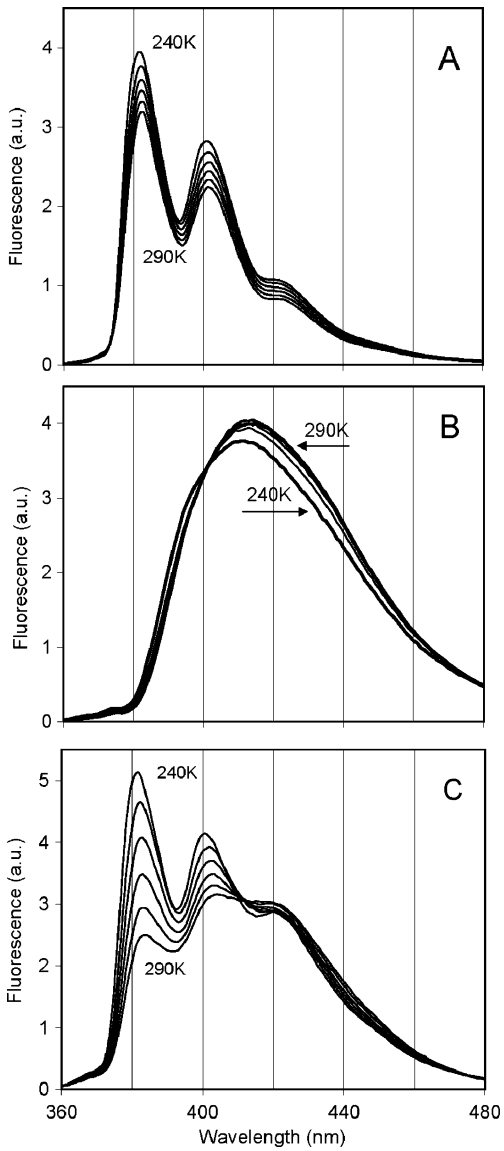

Fig. 6 Effect of temperature from 240–290 K on protonation as indicated by fluorescence emission spectra. **a** Pyrene-1-COO^- in 1/1 (*v*/*v*) glycerol/water pH 9.5, **b** pyrene-1-COOH in 1/1 (*v*/*v*) glycerol/water pH 1, **c** pyrene-1-COO^- in 1 M phosphate pH 5 in 1/1 (*v*/*v*) glycerol/water i.e., 0.21 mol fraction. Spectra taken at temperature increments of 10°

used to calculate bimolecular rate constants based on literature viscosity data, and these data are also plotted in Fig. 7. The rates for proton transfer from phosphate are higher than predicted from simple diffusion. The values for ΔE are 2.7, and 3.9 Kcal/mol for the reaction of H_3PO_4 in water and glycerol/water, respectively. These respective values are 1.8 kcal/mol and 5.1 kcal for acetic acid.

The calculated rate constants based upon viscosity are not rigorously linear in the Arrhenius plot of Fig. 7. The Arrhenius equation assumes a single activated intermediate. In the case of glycerol/water solutions, there is likely to be a distribution of barriers that determine viscosity.

To summarize the above: the ability of phosphate and acetate to transfer protons to the excited state fluorescent molecule is slowed by glycerol. The data presented in Fig. 7 indicates that phosphate is more active than predicted from the Stokes relationship for proton transfer.

Proton transfer and the presence of water in sugar glass

The next experiments were undertaken to attempt to abolish translational diffusion, but to retain a H-bonding network. Optically transparent sugar glasses were prepared that

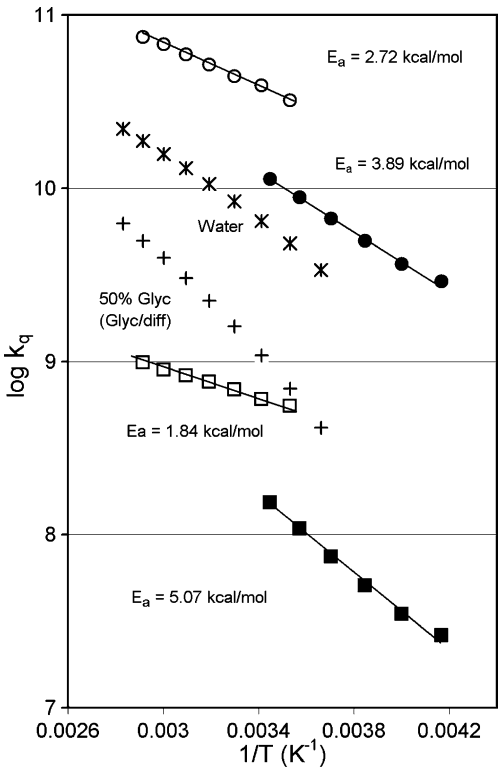

Fig. 7 Arrhenius plot of the bimolecular rate constant for the reaction between excited state pyrene-1-COO^- and phosphate (*circles*), acetate (*squares*). Solvent was water for *open symbols* and 1/1 (*v*/*v*) glycerol/water for *closed symbols*. Diffusion rates in water (*asterisks*), and 50% glycerol (*crosses*) calculated based on viscosity data from the "Handbook of Chemistry and Physics" [36] and Eq. 5. Units of k_q are per molar per second

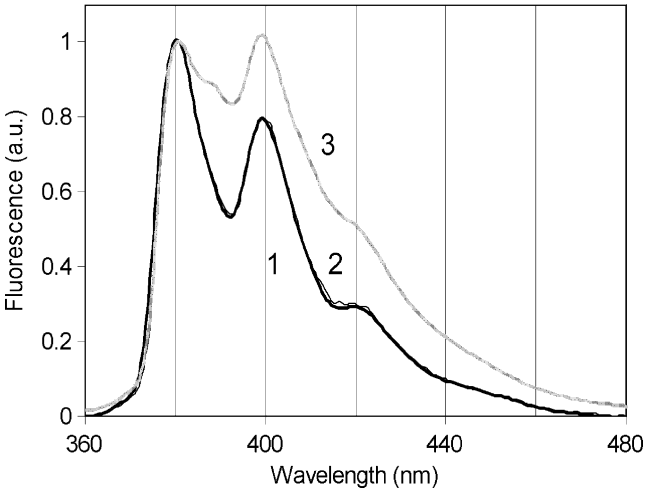

Fig. 8 Fluorescence emission spectra of pyrene-1-COO^- in water-free trehalose/sucrose sugar glass: (*1*) no dopant, (*2*) with sodium acetate and (*3*) sodium phosphate. The mole ratio of sugar to salt was 2/1

contain two disaccharide molecules/molecule of acetate or phosphate. As indicated in "Materials and methods", infrared spectroscopy can tell us the ratio of the glass components. The sugar glasses were dry (no detectible water by IR) or hydrated with water (~1 water/1 sugar molecule). Figure 8 shows emission spectra of pyrene-1-COO^- in trehalose/sucrose glass. No proton transfer was seen in glass that was dry with no added phosphate or acetate (curve 1) or dry glass containing acetate (curve 2). We also examined the spectra of pyrene-1-COO^- in hydrated glass that had no dopant or contained Na-acetate salt. These spectra are not shown but were identical to curve 1 and 2 in that they indicated that no proton transfer occurred during the excited state lifetime. In contrast, as shown by the spectrum in curve 3, when phosphate is present, protonation occurs during the excited state lifetime of the probe.

IR spectra of the trehalose/sucrose glass were examined to characterize water in the glass. The IR bending mode of water is shown in Fig. 9. The glass that contained phosphate retained water under conditions of the sample preparation. The sugar/phosphate/water ratio was ~2:1:1.

The peak position of water bending mode reveals information on the bonding of the water molecule [9, 14]. The peak position frequencies of the water-bending mode are listed on Table 2 and plotted as a function of temperature in Fig. 10. In the presence of phosphate, the HOH bending frequency is higher than in hydrated glass or in water over the entire temperature range. Higher frequency is correlated with tighter H-bonding [9]. Table 2 also lists the HOH bending frequency of water in phosphate solutions. The presence of the phosphate salt increases the HOH bending frequency, consistent with stronger H-bonding. The phosphate solution contains Na^+, but it was shown that

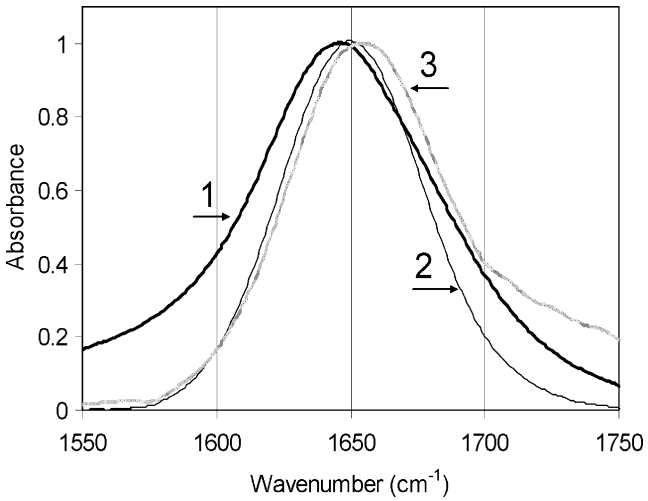

Fig. 9 Normalized IR spectra for HOH bending mode in trehalose/sucrose glass and water. (*1*) water, (*2*) hydrated sugar glass, (*3*) dried sugar glass with phosphate at a 2:1 sugar/salt molar ratio

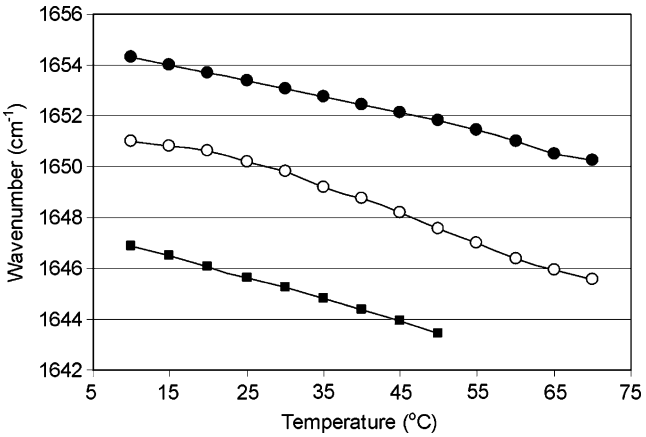

Fig. 10 IR HOH bending mode as a function of temperature. *Closed squares*: neat water; *open circles*: HOH in hydrated trehalose/sucrose glass; *closed circles*: HOH in phosphate containing sucrose glass

NaCl does not alter the IR frequency of water [15], and therefore the shift in the presence of Na phosphate is due to water association with phosphate and is an excellent indication that water is strongly H-bonded to phosphate.

We considered the possibility that acetate might have been lost as acetic acid during the drying procedure. However, this was not the case, since we saw the carboxylate stretching bands in the IR spectrum of the sugar glass (spectrum not shown).

Phosphate infrared spectra

If water is H-bonding strongly to phosphate, phosphate's IR absorption bands should reflect this. IR absorption bands

Table 2 IR absorption peak positions and band-width (full width at half maximum) of HOH bend in liquid and trehalose/sucrose (TS) glass

Conditions	20 °C		60 °C	
	Frequency, cm^{-1}	Fwhm, cm^{-1}	Frequency, cm^{-1}	Fwhm, cm^{-1}
H_2O, bulk	1,646.6	85.4	1,644.6	76.1[a]
Glycerol/water (6/4, *v*/*v*)	1,653.5	73.6	ND	ND
TS hydrated	1,650.6	62.9	1,646.4	56.4
TS-phosphate[b]	1,654.4	61.6	1,650.8	60.0
Na phosphate, 1 M in water[c]				
pH 4	1,648.2	83.3	1,645.9	76.2
pH 9	1,648.3	89.5	1,646.3	79.5
pH 11.3	1,649.9	89.8	1,647.0	79.9

ND Not determined, *FWHM* full width at half maximum
[a] 45 °C
[b] Trehalose/sucrose/phosphate: 1:1:1 molar ratio
[c] Phosphate/water: 1:22 molar ratio

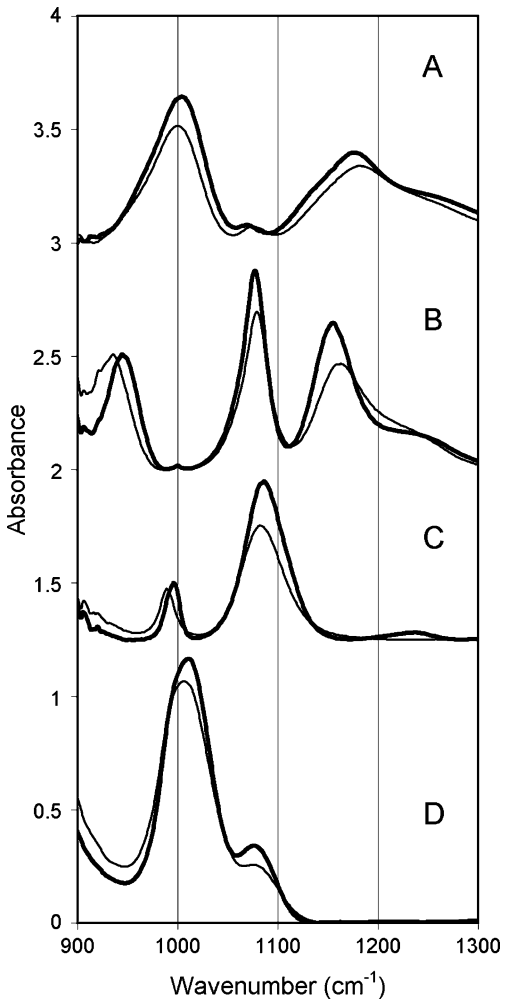

Fig. 11 IR absorption spectra of 2 M sodium phosphate in water measured at different pHs and at 10–20 °C (*thick line*) and 60–70 °C (*thin line*). **a** H_3PO_4, pH 1.2 component of was subtracted. **b** , pH 4.0. **c** pH 9, **d** , pH 11.3. Spacer of the IR cell was 100 μm

involved in H-bonding to water are temperature dependent, unlike most bands [9].

The spectra of all protonated forms of phosphate in HOH are shown for two temperatures in Fig. 11. The temperature dependencies of the major phosphate bands are shown in Fig. 12. Peak positions for phosphate IR absorption, tentative assignments and the frequency differences at two temperatures are given in Table 3. Klahn et al. [16] have calculated the effect of hydration on the IR spectra of phosphate ions in water. For instance, hydration of $H_2PO_4^{-1}$ shifts the calculated frequency of $\nu_a(PO_H)$ from 735 cm^{-1} to higher frequency. If H-bonding to water decreases with increasing temperature, then the temperature dependence of this mode should be negative. In fact, the frequency is lower at higher temperature (Table 2). The temperature dependence of $\nu_a(PO)$ is predicted to be positive based upon the hydration calculations, and this is what is experimentally found.

In summary, the temperature dependence of the IR spectra is consistent with H-bonding between phosphate and water, and decreased H-bonding as temperature increases.

Table 3 IR peak positions for 1 M Na phosphates in water at two temperatures

	Frequency (cm^{-1}) 10 °C	Frequency (cm^{-1}) 70 °C	Δcm^{-1}/deg	Mode, tentative assignment
H_3PO_4	1,171	1,1849	0.215	$\nu_a(PO_H)$
	1,004	9987	−0.088	$\nu_s(PO_H)$
$H_2PO_4^{-1}$	1,155	1,161.3	0.105	$\nu_a(PO)$
	1,077.1	1,078.9	0.030	$\nu_s(PO)$
	944.8	935.3	−0.158	$\nu_a(PO_H)$
	1,197.5	1,204.9	0.123	$\delta_a(PO_HH)$
HPO_4^{-2}	1,081.5	10824	0.020	$\nu_a(PO)$
	991.3	9892	−0.047	$\nu_s(PO)$
	1,233.4			$\delta_a(PO_HH)$
PO_4^{-3}	1,012.8	1,0115	−0.022	$\nu_a(PO)$

Assignments for bending δ and stretching ν modes based upon the work of Klahn et al. [16]. Subscript a refers to antisymmetric; subscript s refers to symmetric.

Discussion

Excited state proton donors, i.e., molecules that become more acidic in the excited state relative to the ground state, have been used in studies of protein and macromolecule surfaces [17–19]. Excited state proton acceptance can also occur during the time-scale of excited states; for instance, aromatic amines become more basic upon excitation [20]. Carboxy-aromatic molecules, as seen in the case of pyrene-1-carboxylate, also become more basic in the excited state and allow study of proton transfer in pH ranges that are relevant for biology [4].

In this work, we examined proton transfer rates when glycerol alters the water matrix. Water/glycerol solutions are widely used to store and study bio-macromolecules, organelles and cells at low temperature [21, 22], and are used experimentally to alter protein dynamics [23–26] and reaction rates [27]. Glycerol itself does not donate a proton to pyrene-1-COO^-*, as was verified by emission spectra.

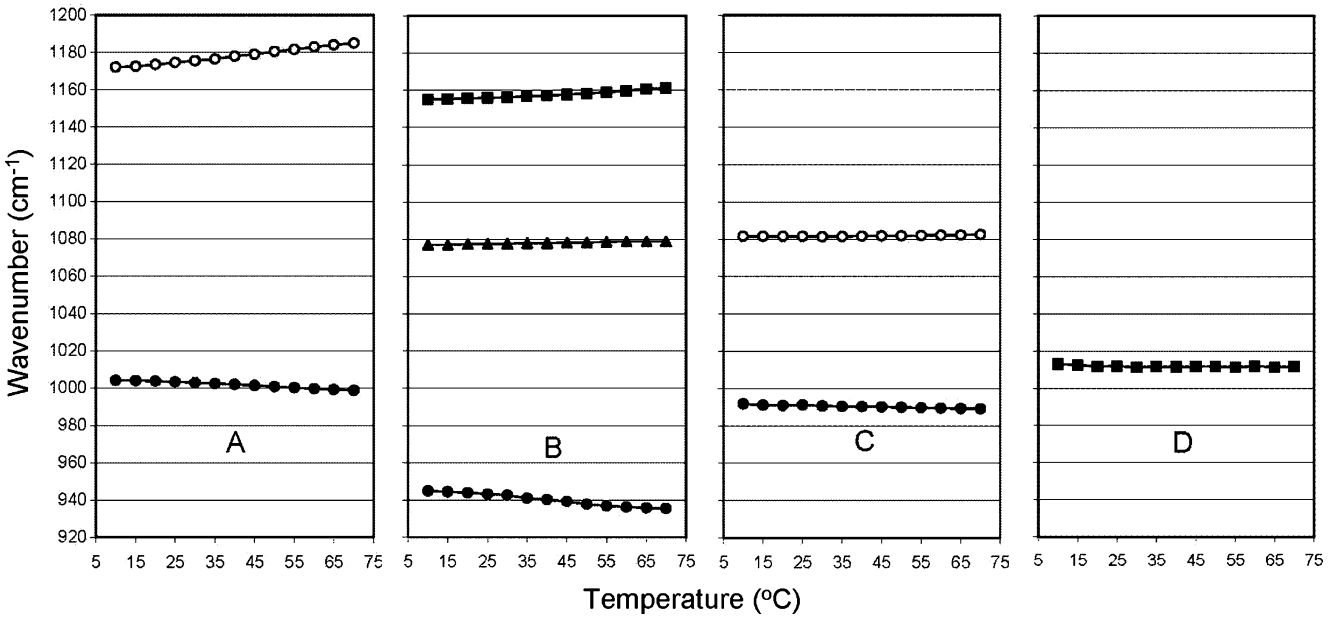

Fig. 12 Temperature dependence of absorption maxima of sodium phosphate. *A* H_3PO_4, pH 1.2: $\nu_a(PO_H)$ *open circles*, $\nu_s(PO_H)$ *closed circles*; *B* pH 4.0: ν(PO) *closed squares*, $\nu_a(PO)$ *closed triangles* and $\nu_a(PO_H)$, *closed circles*; *C* pH 9.0: $\nu_a(PO)$ *open circles*, ν_s (PO *closed circles*); *D* , pH 11.3 $\nu_a(PO)$ *closed squares*

Glycerol has little direct other influences on the excited state molecules as seen by the small dependence of the emission spectra on glycerol (Fig. 2), and the lifetime (Table 1). The pK of phosphate and acetate may change as glycerol is added. A change in pK may alter the rate in two ways. First, the rate is dependent upon the driving force [28]; the rate may change due to this. Second, since, we calculate the amount of H_3PO_4 and acetic acid based upon their pKs, and uncertainty in the pK in glycerol solutions would add a systematic error. However, to circumvent this, the pKs were determined based upon change of pH measured in given glycerol concentrations. The observed difference in rate for diffusion and for phosphate reaction, which is an order of magnitude, cannot be accounted for by possible error in calculation or change in driving force.

Making reasonable assumptions, all based upon experiment, we consider how cosolvent affects proton transfer. One effect of cosolvent is to reduce the rate of proton transfer by reducing diffusion rates of the weak acids that serve as the proton donors. Glycerol solutions are more viscous than pure water and since protonation rates are dependent upon the diffusion of reactants, proton transfer rates are decreased. A second effect is that the presence of cosolvent affects the H-bonding network of water. The diffusion of hydronium in water occurs at rates faster than the diffusion of other cations [29]. Water is both an H-bond donor and acceptor, and it is widely agreed that by changing the H-bond arrangement, protons can be transferred without translational diffusion of water's oxygen atom.

Taking this in mind, we note that the rate of proton transfer decreases about five times in going from water to ~0.8 mole fraction of glycerol at the given phosphate or acetate concentration [Fig. 4). When rate was considered as a function of viscosity, non-linear behavior was seen for both proton donating systems (Fig. 5). In the viscosity range of 1 to 2.5 cP the proton transfer reaction follows the Stokes relationship (Fig. 5a). In this range, there is still a three dimensional network of H-bonds (see Fig. 5b; data based on literature [5, 12, 13]). At higher glycerol concentrations, non-linear dependence on viscosity is seen, consistent with a slowing of the reaction when the H-bonding network is disrupted. Consequently, it appears that when the network of water H-bonding is intact, both diffusive and H-bond assisted components determine the rate.

The dependencies of the rates of protonation by acetic and phosphoric acid show similar dependence upon the glycerol concentration. However, the rate of reaction for phosphate is higher than predicted for two diffusing spheres (Fig. 7). So how can one account for the apparent high proton transfer ability of phosphate? Previous work gave evidence that phosphate ion enhances proton transfer rates in water; the enhanced proton transfer rate is attributed to phosphate's ability, like water, to be both a proton donor and acceptor [4]. At the 1/1 glycerol/water studied, the two dimensional H-bonding network of water is still intact, but, in effect, the rate decreases in part because the effective path-length through the 2-D network is long.

At 1 M phosphate, the average distance between phosphate molecules is 11.8 Å. This distance, along with charge repulsion, suggests that there is no direct phosphate–phosphate interaction. The evidence is consistent with the view that water is involved in the proton transfer reaction of phosphate. In sugar glass, where there is no translational diffusion, proton transfer can occur when phosphate is present (Fig. 8). In phosphate-doped glass, water is retained (Fig. 9). The stretching and bending frequencies of phosphate are temperature dependent; this suggest water/phosphate interactions since as temperature increases, H-bonding between water molecules decreases, and IR frequencies change [9]. Acetate provides a contrast to phosphate; at high acetate concentrations in glass, whether it is hydrated or water free, no proton transfer occurred within the excited state lifetime of the probe.

We speculate on the relevance of results of our paper to proton transport in cells. The possibility of rapid lateral proton transfer on membrane surfaces has long been considered [30–33]. Phospholipids are the major lipid of membranes, and at the membrane surface the phosphate groups in the lipid heads are bonded to water molecules. The surface area of one phospholipid molecule is around 70 $Å^2$ [34]. The average distance between phosphates then is ~7–8 Å. At this distance, proton transfer necessitates the involvement of water, which has also be demonstrated for similar systems [35]. The surface of membranes would therefore be highly conducting to protons with the effective proton network consisting of water and phosphate groups.

In summary, the data presented in this paper suggest that H-bonding interactions between water molecules and phosphate assist in proton transfer.

Acknowledgment This work was supported by NIH grant PO1 GM48130 (J.M.V.), Texas Emerging Technologies Fund (Z.G. and I. G.) and fellowship NIH F31 NSO53399 to NVN. We thank Jennifer Dashnau, Jennifer Greene and Nathan Scott for helpful discussions.

References

1. Agmon N (1995) The Grotthuss mechanism. Chem Phys Lett 244:456–462
2. de Grotthuss CJT (1806) Memoire sur la decomposition de l'eau et des corps qu'elle tient en dissolution a l'aide de 'ectricite galvanique. Ann Chim Phys LVIII:54–74
3. Nucci NV, Zelent B, Vanderkooi JM (2008) Pyrene-1-carboxylate in water and glycerol solutions: origin of the change of pK upon excitation. J Fluoresc 18:41–49

4. Zelent B, Vanderkooi JM, Coleman RG, Gryczynski I, Gryczynski Z (2006) Protonation of excited state pyrene-1-carboxylate by phosphate and organic acids in aqueous solution studied by fluorescence spectroscopy. Biophys J 91(10):3864–3871
5. Dashnau JL, Nucci NV, Sharp K, Vanderkooi JM (2006) Hydrogen bonding and the cryoprotective properties of glycerol/water mixtures. J Phys Chem 110:13670–13677
6. Zelent B, Nucci NV, Vanderkooi JM (2004) Liquid and ice water and glycerol/water glasses compared by infrared spectroscopy from 295 to 12 K. J Phys Chem A 108:11141–11150
7. Wright WW, Baez CJ, Vanderkooi JM (2002) Mixed trehalose/sucrose glasses used for protein incorporation as studied by infrared and optical spectroscopy. Anal Biochem 307(1):167–172
8. Wright WW, Guffanti G, Vanderkooi JM (2003) Protein in sugar and glycerol/water as examined by IR spectroscopy and by the fluorescence and phosphorescence properties of tryptophan. Biophys J 85:1980–1995
9. Vanderkooi JM, Dashnau JL, Zelent B (2005) Temperature excursion infrared (TEIR) spectroscopy used to study hydrogen bonding between water and biomolecules. Biochim Biophys Acta 1749:214–233
10. Fischkoff S, Vanderkooi JM (1975) Oxygen diffusion in biological and artificial membranes determined by the fluorochrome pyrene. J Gen Physiol 65(5):663–676
11. Angulo G, Grampp G, Rosspeintner A (2006) Recalling the appropriate representation of electronic spectra. Spectrochim Acta A 65:727–731
12. Parsons MT, Westh P, Davies JV, Trandum C, To ECH, Chiang WM, Yee EGM, Koga Y (2001) A thermodynamic study of 1-propanol-glycerol-H2O at 25 degrees C: effect of glycerol on molecular organization of H2O. J Sol Chem 30:1007–1028
13. To ECH, Davies JV, Tucker M, Westh P, Trandum C, Suh KSH, Koga Y (1999) Excess chemical potentials, excess partial molar enthalpies, entropies, volumes, and isobaric thermal expansivities of aqueous glycerol at 25 degrees C. J Sol Chem 28:1137–1157
14. Lloyd KG, Banse BA, Hemminger JC (1986) Vibrational analysis of water adsorbed on Pd(100): sensitivity of the isotope shifts of bending modes to the bonding site. Phys Rev B 33:2858–2860
15. Sharp KA, Madan B, Manas ES, Vanderkooi JM (2001) Water structure changes induced by hydrophobic and polar solutes revealed by simulations and infrared spectroscopy. J Chem Phys 114:1791–1796
16. Klahn M, Mathias G, Kotting CN, Schlitter J, Gerwert K, Tavan P (2004) IR spectra of phosphate ions in aqueous solution: predictions of a DFT/MM approach compared with observations. J Phys Chem A 108:6186–6194
17. Shimoni E, Nachliel E, Gutman M (1993) Gaugement of the inner space of the apomyoglobin's heme binding site by a single free diffusing proton II. Interaction with a bulk proton. Biophys J 64:480–483
18. Gepshtein R, Leiderman P, Huppert D, Project E, Nachliel E, Gutman M (2006) Proton antenna effect of the gamma-cyclodextrin outer surface, measured by excited state proton transfer. J Phys Chem B 110:26354–26364
19. Roche CJ, Guo F, Friedman JM (2006) Molecular level probing of preferential hydration and its modulation by osmolytes through the use of pyranine complexed to hemoglobin. J Biol Chem 281:38757–38768
20. Weller A (1961) Fast reactions of excited molecules. Prog React Kinet 1:187–214
21. Douzou P (1977) Cryobiochemistry. An introduction. Academic, London
22. Prabhu NV, Dalosto SD, Sharp KA, Wright WW, Vanderkooi JM (2002) Optical spectra of Fe(II) cytochrome c interpreted using molecular dynamics simulations and quantum mechanical calculations. J Phys Chem B 106:5561–5571
23. Ansari A, Jones CM, Henry ER, Hofrichter J, Eaton WA (1992) The role of solvent viscosity in the dynamics of protein conformational changes. Science 256:1796–1798
24. Kaposi AD, Vanderkooi JM, Wright WW, Fidy J, Stavrov SS (2001) Influence of static and dynamic disorder on the visible and infrared absorption spectra of carbonmonoxy horseradish peroxidase. Biophys J 81(6):3472–3482
25. Kaposi AD, Prabhu NV, Dalosto SD, Sharp KA, Wright WW, Stavrov SS, Vanderkooi JM (2003) Solvent dependent and independent motions of CO–horseradish peroxidase examined by infrared spectroscopy and molecular dynamics calculations. Biophys Chem 106:1–14
26. Stavrov SS, Wright WW, Vanderkooi JM, Fidy J, Kaposi AD (2002) Optical and IR absorption as probe of dynamics of heme proteins. Biopolymers 67:255–259
27. Khajehpour M, Troxler T, Vanderkooi JM (2003) The effect of protein dynamics upon reactions that occur in the heme-pocket of horseradish peroxidase. Biochemistry 42:2672–2679
28. Marcus RA (1968) Theoretical relations among rate constants, barriers, and Bronsted slopes of chemical reactions. J Phys Chem 72:891–899
29. Dashnau JL, Vanderkooi JM (2007) Computational approaches to investigate how biological macromolecules can be protected in extreme conditions. J Food Sci 72:R1–R10
30. Georgievskii Y, Medvedex ES, Stuchebrukhov AA (2002) Proton transport via the membrane surface. Biophys J 82:2833–2846
31. Gabriel B, Teissie J (1993) Proton long-range migration along protein monolayers and its consequences on membrane coupling. Proc Natl Acad Sci USA 93:14521–14525
32. Mezer A, Friedman R, Noivirt O, Nachliel E, Gutman M (2005) The mechanism of proton transfer between adjacent sites exposed to water. J Phys Chem B 109:11379–11388
33. Serowy S, Saparov SM, Antonenko YN, Koziovsky W, Hagen V, Pohl P (2003) Structural proton diffusion along lipid bilayers. Biophys J 84:1031–1037
34. Huang C, Mason JT (1978) Geometric packing constraints in egg phosphatidylcholine vesicles. Proc Natl Acad Sci USA 75:308–310
35. Friedman R, Fischer S, Nachliel E, Scheiner S, Gutman M (2007) Minimum energy pathways for proton transfer between adjacent sites exposed to water. J Phys Chem B 111:6059–6070
36. Lide DR (ed) (2005–2006) CRC handbook of chemistry and physics. CRC Press, Boca Raton